# Oxygen content effect on mechanical behaviour of cp titanium exposed at elevated temperature.

Quentin Sirvin, Damien Texier, Vincent Velay, Daniel Monceau, Benjamin Dod

# OXYGEN CONTENT EFFECT ON MECHANICAL BEHAVIOUR OF CP TITANIUM EXPOSED AT ELEVATED TEMPERATURE.

Quentin Sirvin[1], Damien Texier[1], Vincent Velay[1], Daniel Monceau[2], Benjamin Dod[3].

*1 Institut Clément Ader (ICA) – UMR CNRS 5312 ; Université de Toulouse ; CNRS, IMT Mines Albi, INSA, ISAE-SUPAERO, UPS ; Albi, France.*
*2 CIRIMAT- UMR CNRS 5085, ENSIACET-INPT ; Toulouse, France.*
*2 AIRBUS Operation SAS ; Toulouse, France.*

Ti-based alloys are particularly prone to oxygen dissolution and embrittlement. Oxygen solubility within titanium leads to the formation of an oxygen-diffusion zone (ODZ) during oxidation processes for a depth up to ten times thicker than the oxide layer. The mechanical and oxidation behaviour of the CP-Ti was investigated using micro-tensile testing of 50 to 800 µm-thick pre-oxidized specimens. Pre-oxidation treatments at 700 °C with various exposures have been performed to generate different ODZ thickness/non-affected material (NAM) thickness ratios ranging from 0 to 100%. These investigations aimed to identify the competition between strengthening effects due to oxygen enrichment and the damage development due to oxygen embrittlement using the graded-property material structure composed of different percentages of NAM and ODZ. Mechanical properties of CP-Ti rise with oxidation time except for strain to failure. The extension of the ODZ follow parabolic law with a parabolic constant 20 $\mu m^2.h^{-1}$.

**Keywords:** Commercial pure titanium; oxygen embrittlement; micromechanical tensile testing; gradient of properties; mechanical behaviour.

## 1. Introduction

Titanium alloys are widely used in flying structures due to their interesting specific mechanical properties, i.e. a “high specific mechanical strength over density” ratio (compared to other metallic structural alloys). They also retain good mechanical properties at intermediate temperatures, making them attractive for the manufacture of components exposed at temperatures up to 650 °C. However, beyond the significant oxidation of titanium alloys at these temperatures [1], the high solubility of oxygen in these alloys induces an oxygen-affected diffusion zone (ODZ), a sub-surface region with a brittle behaviour [2]. The ODZ can extend to depths much greater than the thickness of the oxide layer [3,4] and must be considered in the design of these components, both for static and cyclic stresses. ODZ is characterised by a gradient of chemical composition [5], inducing a gradient of mechanical behaviour that can extend over hundreds of micrometres in depth [6]. This change in chemical composition is reported to change the elasto-visco-plastic behaviour of the base material, even for low oxygen content [7–10]. The determination of local mechanical properties within this compositional/property gradient is necessary to refine predictive models of behaviour, damage and service life of thin titanium-alloy components at intermediate temperature.

The ODZ fails in a brittle manner under tensile loading and transverse cracks normal to the loading direction develop on the whole gage section, acting as severe notches in service [11]. Assessing the local mechanical behaviour of the ODZ and predicting its early cracking in various stress amplitude/temperature ranges are central problematics to better implement microstructure-based fatigue criteria in structural design of Ti-alloys components. Tensile tests are generally performed on relative thick specimens, thicker than 500 µm, leading to particularly low ODZ fraction compared to specimen gauge section. The use of thinner samples aims to increase the "surface layer to volume" ratio of materials with a gradient of properties, and thus to facilitate the micromechanical characterization of ODZ, as demonstrated in ref. [12].

The mechanical and oxidation behaviour of the commercially pure titanium (CP-Ti) were investigated using micro-tensile testing on 50 to 800 µm-thick pre-oxidized specimens. Pre-oxidation treatments at 700 °C with various exposure times have been performed to generate different ODZ thickness/non-affected material (NAM) thickness ratios ranging from 0 to 100 %. These investigations aimed to identify separately the thickness effect and the ODZ/thickness ratio effects on the mechanical behaviour of the structures.

## 2. Material and experiments

Commercially pure titanium was supplied in the form of 1.8 mm-thick sheet metal by "All Metal Services". Its chemical weight % composition is T40-0.14O-0.07Fe.

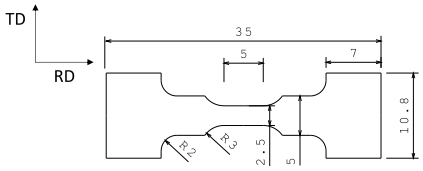


**Figure 1 : Specimen geometry of the micro-tensile specimens (dimensions in mm)**

The as-received material presents a typical α-phase microstructure with an average grain size of 15 µm. The micro-tensile specimens were first machined using water jet technology according to the rolling direction (RD), as defined in Figure 1. The width of the specimen gage was gently rectified for geometrical tolerances but also to minimise the material affected by water jet operation.

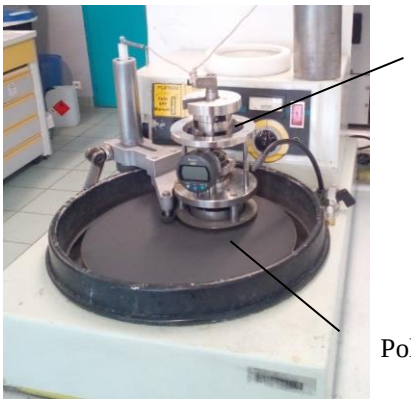


**Figure 2 : Polishing machine and precision Jig**

The micro-tensile specimens were then thinned down on both sides to centre the micro-tensile specimens in the sheet. The thinning protocol was detailed in the work carried out by Texier et al. [13], the aim being to manufacture ultrathin specimens by a gentle mechanical abrasion to ensure adapted geometrical tolerance on centimetre-long samples. The manufacture of such ultrathin specimen requires special know-how and apparatus. For this purpose, a dedicated polishing machine and a precision jig were used, as shown in Figure 2. To assess to the effect of the ODZ on the mechanical integrity of oxidised CP-Ti material, specimens were manufactured at different thicknesses ranging from 50 µm to 1 mm then pre-oxidised at high temperature for different exposure times. It allowed to access to the global mechanical behaviour and quantify the influence of ODZ / NAM ratio, as illustrated in Figure 3.

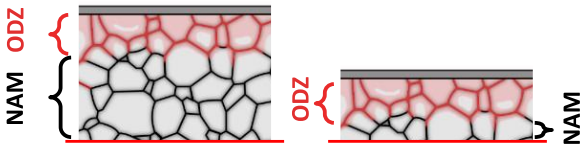


**Figure 3 : Representation of the ODZ / NAM ratio**

A Nabertherm C290 furnace with static atmosphere, i.e. no air stirring, was used for all high temperature pre-oxidation treatments. Loading and unloading operations of micro-tensile specimens were carried out within the hot oven at 700 °C after different durations: 1, 10, 50 and 100 hours. Prior to pre-oxidation, specimens were cleaned in acetone then in ethanol in an ultrasonic bath during 15 minutes each. During pre-oxidation, head samples radii were held on an alumina rod using nickel-chromium alloy hooks (K-type thermocouple wires). The alumina rods were placed on a refractory brick support.

Tensile tests were performed at room temperature on an Instron 5800R electromechanical tensile testing machine using BlueHill2 software. The dedicated micro-tensile testing device is detailed in Figure 4. Load-cells with a load range of either 5 kN or 0.5 kN were used depending on the micro-specimen thickness for higher sensitivity, accuracy and

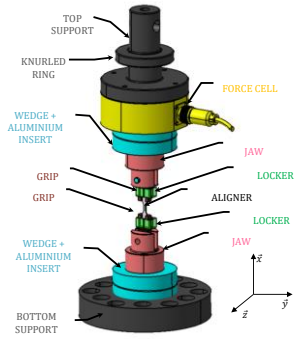


**Figure 4 : Dedicated micro-tensile testing device**

repeatability in results. Tensile properties of titanium alloys are sensitive to strain rate even at room temperature [11], [12]. As the use of classical contact extensometer is not possible for such thin micro-tensile specimens, a non-linear crosshead motion was applied to achieve a constant strain rate $\dot{\varepsilon}$ during tensile tests. This non-linear traverse motion is intended to compensate the stiffness of the tensile line in order to improve the characterization of the elastic to plastic transition of the tested material/specimen. The smooth transition from elastic to plastic-displacement control was ensured using a sigmoidal function detailed in Equation 1. Several calibration tests were performed to identify $\alpha_1$ and $\alpha_2$ parameter as a function of the specimen thickness.

$$v = \dot{\varepsilon}_x + \alpha_1 . \left(1 - \frac{1}{1 + e^{(\alpha_2 - t)}}\right) \qquad \textbf{Equation 1}$$

Digital image correlation techniques were paired to the tensile tests in order to assess to the full-field deformation within the specimen gauge, the macroscopic deformation using optical extensometry, as well as the cracking premises. The image correlation bench consisted of a "Pike 5B/C" camera (5Mpx), a "Sigma DG Macro" lens, a lighting system composed of a "Dedolight" spot and a "KERN Optics" light ring. The acquisition of the images was carried out with VicSnap® software. All data, i.e., time, forces and cross-head displacements, were simultaneously recorded using a National Instrument® USB module for each image acquisition.

Fractographic analyses were performed using a field emission gun - scanning electron microscope (FEG-SEM) Nova NanoSEM 450 from Thermo Fisher Scientific in a secondary electron (SE) mode.

To access to chemical composition, a Cameca SXFiveFE microprobe was used. It allows quantitative analyses of submicron particles for elements ranging from Be to U, i.e. almost the entire periodic classification, with detection limits of about 0.01%. Natural standards were used to quantitatively obtain the oxygen content difference within the ODZ relative to the oxygen content within the NAM by spectrum subtraction [16].

## 3. Results

### 3.1. Mechanical properties

For this study, all the tensile tests were doubled to check the robustness and repeatability of the procedure implemented (specimens named #1 and #2). For stress calculation, ODZ + NAM are considered as the transverse section.

### 3.2. Tensile behaviour of non-oxidized/pre-oxidized specimens

Tensile tests were first conducted on non-oxidised specimens with different thicknesses ranging from 50 to 800 µm for reference and comparison with pre-oxidized specimens. The stress-strain (engineering) curves of the different specimens are depicted in Figure 5(a). All the specimens exhibit a similar tensile behaviour regardless of the specimen thickness, except for the thinnest thickness (50 µm). The thinning specimens show a reduction of about 70 % on the elongation and a slight increase in yield strength of 12 %. This can be attributed to the strain distribution and localisation sensitivity of the material due to geometrical tolerances on the specimen thickness. Specimens exhibit an elastic behaviour up to 300 MPa and a significant work-hardening up to an ultimate tensile strength of 450 MPa reached at 11 % total strain. The stress then gradually decreases with the elongation. The strain-to-failure is about 35 % and 30 % total strain for the thicker specimen (800 µm) and almost thinnest specimen (100 µm). The strain-to-failure decreases with the specimen thickness.

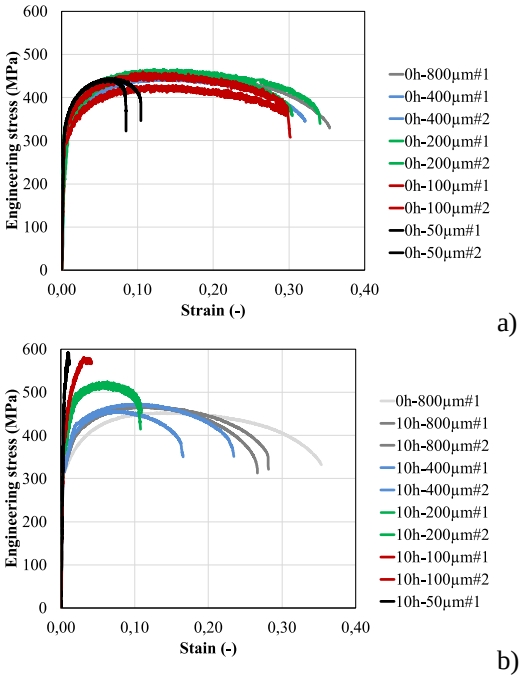


**Figure 5 : Stress-strain curves of (a) non-oxidized specimens and (b) 10h pre-oxidation specimens**

Tensile tests were performed on pre-oxidised specimens and the stress-strain (engineering) curves are shown in Figure 5 (b) for 10 hours of pre-oxidation time. Interestingly, the specimen thickness, and thus the ODZ / NAM ratio, plays an important role in the evolution of the mechanical properties, contrary to what was observed for the "non-oxidised" state. For direct comparison between the non-oxidised state and 10 hours pre-oxidised state, the curve of the non-oxidised 800 µm-thick specimen was taken as a reference (light grey curve in Figure 5 (b)). For an oxidation time of 10 h, the strain-to-failure was reduced by almost 90 % for 100 µm-thick specimens in comparison with the as-received material, showing the deleterious effect of oxygen embrittlement. However, the yield strength and ultimate tensile strength increases significantly up to 20 % showing both the strengthening effect due to oxygen insertion within titanium and the strain localisation effect due to multi-cracking of the ODZ. The evolution of the strain hardening of the material did not follow the same trend. The thinner the specimens, the less important the ductile behaviour of the micro-sample. When increasing the oxidation time, the ductility of micro-tensile specimens at a given thickness decreased. In some cases, no macroscopic plastic domain was observed, attesting the fully brittle behaviour of the highly oxygen-affected samples. For the longest oxidation times, some specimens that could not be tested due to failure during specimen manipulation or even during oxidation.

It is worth reminding that aging of T40 lead to a decrease in yield strength, ultimate tensile strength and strain-to-failure as a function of the aging duration due to slight increase in grain size in the NAM or thickness reduction [9,17]. Conversely, oxidation and oxygen dissolution were found to significantly increase the tensile strength compared to the as-received and aged materials.

Tensile properties in terms of yield strength, ultimate tensile strength, strain-to-failure and Young's modulus are depicted respectively in Figure 6, Figure 7, Figure 8 and Figure 9 for all the specimens and oxidation times.

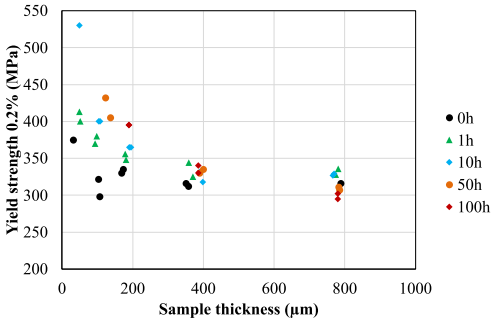


**Figure 6 : Evolution of yields strength with oxidation duration at 700°C and sample thickness**

For the as-received material, the mechanical properties vary little with the thickness except for Young's modulus which tends to decrease by about 16 %. When the material was subjected to oxidation, the evolution of the properties was completely different. For

specimens with a thickness of 800 µm, the yield strength and ultimate tensile strength changed very little. The strain-to-failure decreased by half and the Young's modulus increased about 30 %. For thinner specimens, the trends in strain-to-failure and Young's modulus were identical, i.e. a decrease and increase of the strain-to-failure and the Young's modulus for either a decrease in specimen thickness or increase in oxidation time, respectively. However, there is a strong evolution of the yield strength as well as the ultimate tensile strength which can reach more than 25 %. The yield strength increases as a function of the oxidation time and the thickness of the specimen. Ultimate tensile strength proposes an exponential evolution between 0 to 10 h and a bell-shape form after 50 h to reach a maximum for 400 µm specimen thickness.

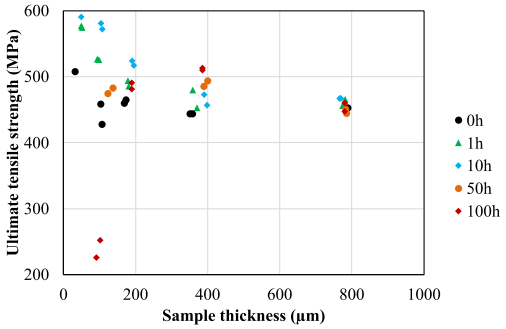


**Figure 7 : Evolution of ultimate tensile strength with oxidation duration at 700°C and sample thickness**

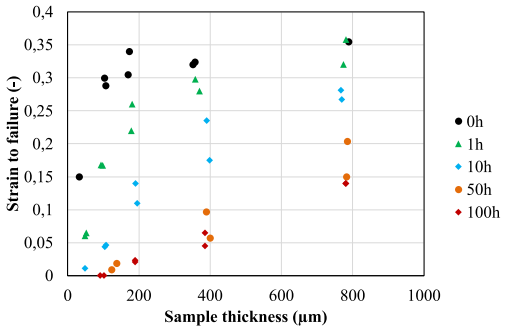


**Figure 8 : Evolution of strain to failure with oxidation duration at 700°C and sample thickness**

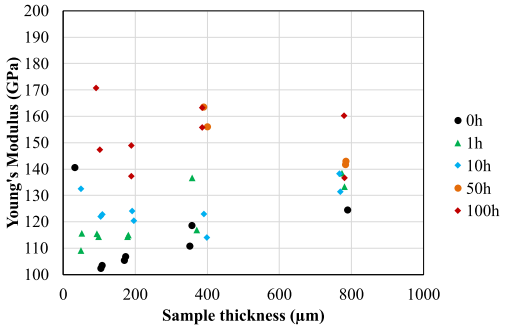


**Figure 9 : Evolution of Young's modulus with oxidation duration at 700°C and sample thickness**

### *3.3. Fracture surface*

Fracture surfaces were observed for all the tested specimens. Figure 10 shows the fracture surface for 100 µm-thick samples and three oxidation times (0 h, 50 h, 100 h) at 700 °C. The measurement of the thickness of the affected zone on a fracture surface is relatively complex to perform due to the subjectivity of this analysis (brittle/ductile transition, necking, etc.). However, the evolution of the brittle zone is about 0 µm (0%) for the 0 h, 33µm (65%) for 50 h, and 100µm (100%) for 100 h. For pre-oxidized specimens, the fracture surface is divided into two regions, i.e. a ductile zone in the core of the specimens surrounded by a brittle region corresponding to the ODZ (Figure 7 b) and c)). The evolution of the ODZ increases with the pre-oxidation time as a parabolic law, the ODZ after 50 h oxidation time being roughly three times thicker than the ODZ after 10 h oxidation. It is interesting to see that for an oxidation time of 50 h the core region remains ductile (around 35%) whereas for a 100 h oxidation time the surface fracture is completely brittle.

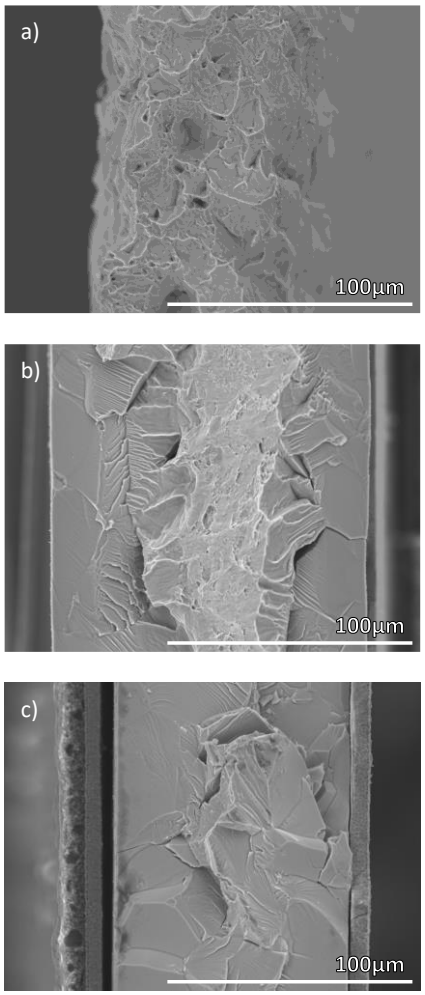


**Figure 10 : Fracture surface for 100 µm thickness specimens and different oxidation durations: a) 0 h, b) 50 h, c) 100 h**

### *3.4. Chemical analysis*

EPMA analysis allows to quantitatively measure the element composition on transversal cutting (atomic %). For each analysis, four profiles were carried out. Due to passivation of titanium at room temperature, the O content was measured relative to a reference state, i.e. the NAM, by spectrum subtraction of O. Oxygen profiles measured on the 100 µm-thick specimens followed an *erf* function as a function of the distance from the metal/oxide interface due to solid state diffusion of O within Ti. Oxygen profiles were fitted and the extension of the ODZ was considered as the depth at a difference of oxygen content of 0.5 %at. more than NAM oxygen concentration. The ODZ extension was found of 0, 6, 15, 30 and 45 µm for 100 µm-thick specimens for 0, 1, 10, 50, and 100 h pre-oxidation duration, respectively. It is interesting to note that the ODZ thickness grows with parabolic kinetics, i.e. $e^2 = k_p.t$ with a value of $k_p = 20$ µm².h$^{-1}$. Finally, the maximum oxygen concentration measured at the metal/oxide interface never exceeded 30 at. %, below 33 at. %, the oxygen solubility limit within α-titanium in pure oxygen.

## 4. Discussion

The influence of the oxidation duration as well as the specimen thickness on the mechanical behaviour of a commercially high purity titanium (T40) was clearly demonstrated using ultrathin specimens with high ODZ / NAM thickness ratio. The mechanical properties of the material such as yield strength and Young's modulus, increase as a function of the oxidation time and the thickness of the specimen. On the other hand, ultimate tensile strength proposes a bell-shaped evolution, with a drop in properties for specimen thicknesses below 400 µm and beyond 50 h of oxidation time. About the ductility properties, strain to failure is greatly reduced when increasing the oxidation duration, and the ductility increases proportionally to the thickness. Between the two extreme treatment times (0h and 100h), an increase of 5 % is observed on the yield strength for 800 µm-thick specimens while it is more than 15 % 200 µm-thick specimens. On the other hand, the strain to failure will be reduced by approximately 80 % regardless of the thickness. Similarly, the yield strength of the material is improved by almost 25 % for two specimens with thickness of 800 and 200 µm for a 100 h treatment. However, the strain to failure is impaired by 60 %. In other words, an increase in tensile properties will inevitably result in a reduction in the ductility of the material.

During the oxidation treatment, the extension of the so-called oxygen diffusion zone (ODZ) becomes more and more important compared to the total thickness of the specimen. As shown by Vaché et al. [4] in his review and modeling, and Casadebaigt [18], the progression of the brittle zone is parabolic, and the kinetic constant follows an Arrhenius law that has the same activation energy as the O. This zone is well known to exhibit a brittle behaviour under tensile loading for concentration higher than 0.5 at. %. [6,19,20] but also, a solid-solution strengthening effect.

The insertion of oxygen into Ti-6Al-4V, even in small proportion, impairs the mechanical properties of the material [21] due to change in the dislocations motion [22]. Many studies have focused on these observations using different oxygen loading techniques. These techniques consist in either carrying out an oxidation operation at high temperature [23–26] or by using alloys with different oxygen levels [7,27–29].

For pure titanium the solid-solution strengthening has been reported for tensile tests performed at room temperature for less than 0.5 at. %., i.e. 5,000 at.ppm oxygen, on massive titanium alloys specimens [20,22]. For higher oxygen concentration, the brittleness of the "oxygen-rich" specimens lead to a lack of data in the open literature. However, the solid-solution strengthening effect was demonstrated using micro-hardness measurements in a compressive way. In the present study, we were capable to evidence the solid-solution strengthening effect under tensile experiments using ultrathin specimens with a significant ODZ compared to the gauge section with a gradient of oxygen concentration varying from 25 % at the metal/oxide interface to 0.14 % in core. Similar increase in yield strength as well as the ultimate tensile strength and modulus increase was only reported in the literature for pure titanium at elevated temperature (CP-Ti50) [6,27–29]. For Ti-alloys, the same tendency in ductility loss is observed but a drop in mechanical properties occurred for Ti-alloys as the proportion of oxygen increases. This difference in mechanical response for Ti-alloys arises from a higher sensitivity to notches [5,21]. Early damage development in the ODZ for Ti-alloys is sufficient to occult potential strengthening effects due to oxygen insertion. For CP-Ti, the work-hardening and ductility are sufficiently important to evidence the solid-solution strengthening effect under tension for high oxygen concentration at the metal/oxide interface.

## 5. Conclusions

The influence of the oxygen dissolution with particularly high oxygen content on the macroscopic tensile properties of a CP-Ti was evidenced. The extension of the ODZ follow parabolic law with a parabolic constant 20 µm².h$^{-1}$. All the mechanical properties i.e. yield strength, ultimate tensile strength and Young's modulus increase with the ratio of ODZ / NAM up to a critical ODZ fraction, attesting the competition between O strengthening and O embrittlement on such property-graded materials.

## 6. Acknowledgements

The authors are particularly grateful to AIRBUS company for the financial support. This work was supported by the Agence Nationale de la Recherche (ANR) [ANR-18-CE08-0003; ANR-JCJC-COMPAACT project funded from the AAPG2018]. The authors are

grateful to Sophie GOUY from the Raymond Castaing Microanalysis Centre (Mixed Services Unit 3623) for access to microscopy facilities and assistance. 

## 7. References


1. M. Peters, J. Kumpfert, C. H. Ward, and C. Leyens, Advanced Engineering Materials **5**, 419 (2003)
2. G. Baur and P. Lehr, Journal of the Less Common Metals **69**, 203 (1980)
3. P. A. J. Bagot, A. Radecka, A. P. Magyar, Y. Gong, D. C. Bell, G. D. W. Smith, M. P. Moody, D. Dye, and D. Rugg, Scripta Materialia **148**, 24 (2018)
4. N. Vaché and D. Monceau, Oxidation of Metals **93**, 215 (2020)
5. J. Baillieux, D. Poquillon, and B. Malard, Philosophical Magazine Letters **95**, 245 (2015)
6. J. Baillieux, Effet de l'oxydation Sur Le Comportement Mécanique de Structures Minces En Alliages de Titane, phd, 2015
7. B. F. Vicente, R. N. D. Correa, A. G. T. Donato, E. V. Arana-Chavez, A. R. M. Buzalaf, and R. C. Grandini, Materials **7**, (2014)
8. H. Hornberger, C. Randow, and C. Fleck, Materials Science and Engineering: A **630**, 51 (2015)
9. W. L. Finlay and J. A. Snyder, JOM **2**, 277 (1950)
10. M. Yan, W. Xu, M. S. Dargusch, H. P. Tang, M. Brandt, and M. Qian, Powder Metallurgy **57**, 251 (2014)
11. G. R. Yoder, L. A. Cooley, and T. W. Crooker, MTA **8**, 1737 (1977)
12. C. Romain, D. Texier, C. Desgranges, J. Cormier, S. Knittel, D. Monceau, and D. Delagnes, Oxidation of Metals **96**, 169 (2021)
13. D. Texier, D. Monceau, J. C. Salabura, R. Mainguy, and E. Andrieu, Materials at High Temperatures **33**, 325 (2016)
14. A. Majorell, S. Srivatsa, and R. C. Picu, Materials Science and Engineering: A **326**, 297 (2002)
15. S. Hémery and P. Villechaise, Materials Science and Engineering: A **697**, 177 (2017)
16. C. Dupressoire, A. Rouaix-Vande Put, P. Emile, C. Archambeau-Mirguet, R. Peraldi, and D. Monceau, Oxid Met **87**, 343 (2017)
17. A. Casadebaigt, J. Hugues, and D. Monceau, Corrosion Science **175**, 108875 (2020)
18. A. Casadebaigt, Etude de l'oxydation à Chaud d'échantillons En Alliage TA6V Élaborés Par Fabrication Additive. Conséquences Sur Les Propriétés Mécaniques., 2020
19. F. Geng, M. Niinomi, and M. Nakai, Materials Science and Engineering: A **528**, 5435 (2011)
20. Q. Yu, L. Qi, T. Tsuru, R. Traylor, D. Rugg, J. W. Morris, M. Asta, D. C. Chrzan, and A. M. Minor, Science **347**, 635 (2015)
21. D. Texier, Q. Sirvin, V. Velay, M. SALEM, D. Monceau, B. Mazères, E. Andrieu, R. Roumiguier, and B. B. Dod, in *Ti2019: The 14th World Conference on Titanium* (Nantes, France, 2019)
22. N. Chaari, D. Rodney, and E. Clouet, Scripta Materialia **162**, 200 (2019)
23. H. L. Du, P. K. Datta, D. B. Lewis, and J. S. Burnell-Gray, Oxid Met **45**, 507 (1996)
24. H. L. Du, P. K. Datta, D. B. Lewis, and J. S. Burnell-Gray, Corrosion Science **36**, 631 (1994)
25. P. Kofstad, Journal of the Less Common Metals **12**, 449 (1967)
26. J. Unnam, R. N. Shenoy, and R. K. Clark, Oxid Met **26**, 231 (1986)
27. B. Barkia, V. Doquet, J. P. Couzinié, I. Guillot, and E. Héripré, Materials Science and Engineering: A **636**, 91 (2015)
28. J.-P. Couzinie, B. Barkia, V. Doquet, and I. Guillot, in (Jackson Lake, United States, 2012), p. pp.411-419
29. B. Sun, S. Li, H. Imai, T. Mimoto, J. Umeda, and K. Kondoh, Materials Science and Engineering: A **563**, 95 (2013)